Heliyon 10 (2024) e34968

Contents lists available at ScienceDirect

Heliyon

journal homepage: www.cell.com/heliyon

Research article

JDF promotes the apoptosis of M2 macrophages and reduces epithelial-mesenchymal transition and migration of liver cancer cells by inhibiting CSF-1/PI3K/AKT signaling pathway

Xiaolin Liu [a], Zongyao Wang [b], Xiang Lv [a], Zhihui Tao [c], Liubing Lin [a], Shasha Zhao [a], Kehui Zhang [a], Yong Li [a,*]

[a] Shanghai Municipal Hospital of Traditional Chinese Medicine, Shanghai University of Traditional Chinese Medicine, Shanghai 200071, China
[b] Sartorius Stedim (Shanghai) Trading Co., Ltd, Shanghai 201210, China
[c] Seventh People's Hospital of Shanghai University of Traditional Chinese Medicine, Shanghai 200137, China

ARTICLE INFO

Keywords:
JDF
M2 macrophages
CSF-1/CSF-1R/PI3K/AKT
Epithelial-mesenchymal transition
Migration and invasion
Liver cancer

ABSTRACT

Background: The interaction between cancer cells and the tumor microenvironment is of critical importance in liver cancer. Jiedu Granule formula (JDF) has been shown to minimize the risk of recurrence and metastasis following liver cancer resection. Investigating the mechanism underlying the therapeutic effects of JDF can extend its field of application and develop novel treatment approaches.

Methods: We established a rat liver orthotopic transplantation tumor model, and recorded the prognostic effects of JDF adjuvant therapy on the recurrence and metastasis of liver cancer. Liver and lung tissues were collected for immunofluorescence staining and H&E staining, respectively. In addition, THP-1 cells were incubated with PMA and IL-4 to induce them to differentiate into M2 macrophages. CSF-1 expression was knocked down using lentivirus to determine the function of CSF-1. Liver cancer cells were cultured with a conditioned medium (CM) or co-cultured with macrophages. Cell viability was determined using the MTT assay. The levels of CSF-1, CSF-1R, E-cadherin, N-cadherin, PI3K, AKT, and cleaved caspase-3 were detected using ELISA, Western blotting and qPCR. The ability of cells to migrate was assessed using cell scratch and transwell assays. Apoptosis was evaluated using flow cytometry.

Results: The JDF treatment decreased the risk of liver cancer metastasis after surgery and the infiltration of CD206/CD68 cells in liver cancer tissue. In cell experiments, JDF showed effects in suppressing M2 macrophages activity and downregulating the expression of CSF-1 and CSF-1R. The concentration of CSF-1 in the supernatant was also lower in the JDF-treated group. Furthermore, M2-CM was found to promote cancer cell migration and epithelial-mesenchymal transition (EMT); however, these effects were weakened after administering JDF. Knocking down endogenous CSF-1 in M2 macrophages resulted in a comparable suppression of cancer cell migration and EMT. Additionally, JDF treatment inhibited activation of the PI3K/AKT pathway, thus promoting the apoptosis of M2 macrophages.

Conclusions: Treatment with JDF reduced the EMT and migratory capacity of liver cancer cells, which might be attributed to the inhibition of M2 macrophage infiltration and interruption of the

* Corresponding author. Shanghai Municipal Hospital of Traditional Chinese Medicine, Shanghai University of Traditional Chinese Medicine, No. 274 Zhijiang Middle Road, Jing'an, Shanghai 200071, China.
E-mail address: liyong@shutcm.edu.cn (Y. Li).

https://doi.org/10.1016/j.heliyon.2024.e34968
Received 28 February 2024; Received in revised form 16 July 2024; Accepted 19 July 2024
Available online 2 August 2024

CSF-1/PI3K/AKT signaling pathway. This mechanism may hold significant implications for mitigating the risk of metastatic spread in the aftermath of hepatic surgery.

1. Introduction

Liver cancer, which was ranked as the third deadliest form of malignant tumors globally, with an estimated over 800,000 new cases and more than 700,000 deaths projected for 2022 [1]. It exhibits the fastest growth rate and has a meager five-year overall survival (OS) rate of only 18 % for all stages combined [2]. Treatment options for liver cancer are limited. Although surgical resection is a recommended method for treating early-stage liver cancer, the high recurrence rate and low survival rate after surgery are unsatisfactory [3–5].

Various adjunct therapeutic methods, including transarterial chemoembolization (TACE) [6], interferon therapy [7], chemotherapy [8], and adoptive immunotherapy are employed clinically to prevent recurrence following resection. Traditional herbal medicine (THM) is considered the culmination of Chinese national wisdom and is widely used in Asia to improve the prognosis of cancer patients [9,10]. Jiedu Granule formula (JDF) is an empirical formula developed by Professor Changquan Ling based on the 'cancer poison theory'. Its active components have shown strong antitumor activity [11]. The serum containing *Pseudobulbus Cremastrae* seu Pleiones inhibits the ability of SMMC-7721 cells to adhere and invade [12]. *Salvia chinensis* Benth and the bulb of *Cremastra appendiculata* show antiangiogenic and cytotoxic properties against liver cancer cells [13]. *Actinidia chinensis* root extract (acRoots) shows anti-hepatocellular carcinoma activity via EP3 [14]. JDF has anti-inflammatory effects. The intervention of JDF is beneficial for the prevention and treatment of fever and hepatic pain in patients after TACE [15]. Furthermore, long-term follow-up studies indicate that JDF can prolong the disease-free survival and overall survival of postoperative patients with liver cancer [16,17]. However, the mechanism by which JDF prevents postoperative recurrence and metastasis of liver cancer remains unclear, which greatly limits its wide clinical application.

The liver is an essential metabolic organ in the human body, possessing robust innate immunity. During the development of liver cancer, caused by chronic inflammation, extensive changes occur in the composition and biological functions of innate immune cells [18]. Critical to the immune response, macrophages are recruited to the affected area; however, their function can be highly adaptable under different conditions. Activated macrophages are generally categorized as either M1 or M2 subtypes based on the different markers present [19]. In contrast to M1 phenotype, M2 macrophages possess anti-inflammatory properties and are responsible for supporting angiogenesis while suppressing immune responses in the tumor microenvironment (TME), thereby promoting tumor progression and distant organ metastasis [19,20]. Most tumor-associated macrophages (TAMs) exhibit M2-like macrophage characteristics. Driving the polarization of M2 macrophage strongly promotes the development and *in vivo* metastasis of liver cancer [21,22]. Currently, there is ongoing research on deciphering the mechanism of the interaction between liver cancer cells and TAM, which holds promise as a novel and efficacious therapeutic strategy.

Colony stimulating factor (CSF-1/M-CSF) is believed to have a vast range of effects on myeloid cell maturation; it promotes the growth of macrophages and osteoclast. Its influence on target cells is mediated through the CSF-1 receptor (CSF-1R) [23]. The high expression of CSF-1 is an indicator of a poor prognosis [24], and is widely associated with enhanced invasion. Patients with metastatic hepatocellular carcinoma usually experience an anti-inflammatory state. Specifically, higher levels of CSF-1, along with an increased presence of Th2 cytokines and a decreased presence of Th1 cytokines, are found in the metastasis-inclined microenvironment sample [25]. The CSF-1/CSF-1R pathway may play a crucial role in the postoperative metastasis of liver cancer.

By conducting preliminary studies on rats, we confirmed that JDF can reduce the risk of postoperative metastasis of liver cancer to a certain extent. The rats treated with JDF exhibited a lower infiltration of CD206/CD68 cells in their cancerous tissue. Taking all of these considerations into account, we propose the following hypothesis: JDF may influence the motility potential of liver cancer cells, including processes such as epithelial-mesenchymal transition (EMT), migration, and invasion, by modulating M2 macrophages. The objective of this study is to investigate the effect of JDF on macrophages and liver cancer cells.

2. Materials and methods

2.1. Animals

2.1.1. Establishment of a postoperative model of rat liver cancer and drug administration

All experiments were approved by the Ethics Committee of experimental animal medicine of Shanghai Hospital of Traditional Chinese Medicine (Approval No.: 2020002). Wistar rats (102, Charles River Laboratories, Beijing, China) were used to construct the animal model, as illustrated in Fig. S1. The rat liver fibrosis model was established using dimethylnitrosamine (DMN; D0761, TCI Co., Tokyo, China) [26], whereas the rat liver cancer model was established by orthotopic carcinoma transplantation [27]. After the resection of hepatocellular carcinoma, rats were administered JDF via oral gavage, and their general condition, along with the recurrence and metastasis of cancer, were monitored. The samples of lung tissue and liver tissue were collected and preserved.

2.1.2. Establishment of rat liver fibrosis model

The DMN was diluted with normal saline to create a concentration of 0.5 %. Then, the rats were injected with 1.33 mL/kg DMN intraperitoneally every other day for three times a week during the first and second weeks. In the third week, the rats were injected

with 1.00 mL/kg DMN every other day, again for three times a week. In the fourth week, the rats were injected with 0.60 mL/kg DMN every other day for three times a week. After constructing the model, rats were randomly selected for Sirius red staining and H&E staining to confirm whether the fibrosis model was successfully established (Figure S1 a-b).

2.1.3. Establishment of rat liver orthotopic transplantation tumor model

Initially, a suspension of Walker 256 cells (1×10^7 cells) obtained from Tong Pai Technology in Shanghai, China, was injected into the groin of the right lower limb of female Wistar rats. After the tumor-bearing rats developed a subcutaneous tumor of approximately 2 cm in diameter (usually in 7 days), the subcutaneous tumor was removed and cut into small sections (1 mm^3). Next, using the liver tunnel implantation technique, the tumors were implanted at the same location on the left lobe of the liver, and then, the abdomen was closed by suturing.

2.1.4. Implementation of hepatocellular carcinoma resection in rats and intervention of JDF

Hepatocellular resection was performed 7 days after orthotopic transplantation. The rats were randomly divided into four groups, including the Control group, the low JDF group (JDF-L, 12.74 g/kg/day), the medium JDF group (JDF-M, 38.22 g/kg/day), and the high JDF group (JDF-H, 63.70 g/kg/day). JDF (Actinidia valvata Dunn: *Salvia chinensis* Benth: *Pseudobulbus Cremastrae* seu Pleiones: the gizzard membrane of *Gallus gallus domesticus* Brisson = 3:3:1:1) was prepared by Lei Yunshang Pharmacy in Shanghai, China. From the third day after surgery, rats in the Control group were administered normal saline intragastrically, while the rats in the administration group received JDF treatment at varying concentrations for two weeks. Throughout the study, no rat died because of cancer.

2.2. H&E staining

Freshly collected lung tissue samples underwent an alcohol-paraffin specimen preparation procedure after fixation, and then sectioned for histological analysis. The samples were stained using an H&E staining kit (C0107, Beyotime, Shanghai, China). Hematoxylin solution was utilized to stain the slides for 7 min, followed by staining with the eosin solution for 2 min. Photographs of representative sites were captured with identical parameters.

2.3. Cells

2.3.1. M2 polarization of THP-1 cells

THP-1 cells, obtained from EK Bioscience (CC–Y1519, Shanghai, China), were cultured in RPMI 1640 medium (01-100-1ACS, Biological Industries, Kibbutz Beit Haemek, Israel) supplemented with 10 % fetal bovine serum (FBS; C04001-500, Biological Industries) at 37 °C, and 5 % CO_2 (Forma 371, Thermo, Madison, WI, USA). As previously reported [28], 1×10^6 THP-1 cells in the middle stage of logarithmic growth were seeded in a six-well plate and exposed to a final concentration of 320 nM PMA (phorbol 12-myristate 13-acetate; 16561-29-8, Sigma, St Louis, MO, USA) for 6 h, followed by incubation for 18 h with 20 ng/mL human IL-4 (ab155733, Abcam, Cambridge, MA, USA). The cell morphology and growth were observed under a microscope (CKX3-SLP, Olympus Corporation, Tokyo, Japan).

2.3.2. Construction of a stable CSF-1 gene silenced cell line

The cDNA oligonucleotides repressing CSF-1 were synthesized and inserted was ligated into shRNA lentivirus expressing vector pLV3/H1/GFP&Puro (GenePharma, Shanghai, China). Next, Lipofectamine 2000 (11668019, Invitrogen, Billerica, MA, USA) was used to transfect 293T cells (CC–Y1010, Ek-Bioscience, Shanghai, China). Viruses were collected 48 h post-transfection and used to infect THP cells (MOI:30). The blank vector was used as the negative control (Scramble). A fluorescence microscope (RVL-100-G; ECHO, California, San Diego, USA) was used to observe the growth of stable rotary clones. Subsequently, M2 polarization of ShCSF-1 cells was performed.

2.4. Preparation of JDF solution

The JDF freeze-dried powder was prepared by Shanghai Ronghe Technology Development Co., Ltd. (Shanghai, China). First, the JDF lyophilized powder was ground to a fine powder in a mortar and filtered through a 200-mesh sieve. Then, using a precision electronic balance (ME104E, METTLER TOLEDO, Shanghai, China), 1 g of the filtered powder was weighed and transferred to a 50 mL centrifuge tube. Next, 1 mL of DMSO (D2650, Sigma) and 15 mL of culture medium were added sequentially to ensure the complete dissolution of JDF. The mixture was centrifuged at 3000 rpm for 15 min, and the resulting supernatant was collected. This supernatant was then filtered through a 0.22 μm filter, and the final volume was adjusted to 20 mL, with a solvent concentration of 50 mg/mL. Finally, the solution was packaged and frozen.

2.5. Cell viability assay

To evaluate the half-inhibitory concentration (IC50) of JDF, an MTT kit (M1020, Solarbio, Beijing, China) was used to test cell viability. JDF solution was added to the culture medium with final concentrations of 2 mg/mL, 2.5 mg/mL, 3 mg/mL, 3.5 mg/mL, 4 mg/mL, 4.5 mg/mL, and 5 mg/mL. The suspended cells (1×10^5) were seeded in a six-well plate with JDF. After 24-h incubation, 10 μL of MTT was added to reaction for 4 h, followed by dissolution with Formazan solution. The optical density (OD) value at 490 nm (1510,

Thermo) was measured. A blank control group consisting solely of medium, JDF, and MTT reagent was used to serve as background corrections.

2.6. Preparation of conditioned medium (CM)

The M2 macrophages or shCSF-1 M2 macrophages were cultured in a complete culture medium containing 10 % FBS for 24 h. The supernatant was collected and labeled as M2-CM (M2) or SHCSF-1-CM (shCSF-1), respectively.

The M2 macrophages or shCSF-1 M2 macrophages were cultured in a medium consisting of JDF medium with a final concentration of 3 mg/mL for 24 h. Following this, the supernatant was discarded, and the macrophages were collected. These cells were then cultured for another 24 h in a complete medium containing 10 % FBS to obtain the supernatant. This supernatant was labeled as JDF-CM (JDF) or JDF-shCSF-1-CM (JDF-shCSF-1) accordingly.

2.7. Cell migration

To assess the migratory capacity of cells, we performed cell scratch experiments and transwell assays. MHCC-97H, which are human liver cancer cells with a high metastatic potential, were obtained from EK Bioscience (CC–Y1613). The MHCC-97H cells (5×10^5 cells) were seeded in a 24-well plate and cultured in CM (M2-CM/shCSF-1-CM/JDF-CM/ShCSF-1-JDF-CM) at 37 °C for 24 h. In the scratch assay, when the MHCC-97H cells covered the entire well of the culture plate, a vertical line was drawn at the center using a pipette tip, and the serum-free basal medium was replaced to incubate the cells for 24 h. As for the transwell assay, the re-suspended MHCC-97H cells (5×10^4 cells) were seeded on the upper chamber of the transwell plate, while the lower chamber was filled with serum-containing culture medium and incubated at 37 °C. After 24 h, the migrated cells were fixed and stained for crystal visualization (C02121, Beyotime). Photographs of representative sites were captured with identical parameters.

2.8. Co-culture

The CSF-1 gene-silenced stable cells were seeded in the lower chamber of the transwell plate at a density of 5×10^5 cells/mL and induced the formation of M2 macrophages. Subsequently, the MHCC-97H cells in the logarithmic growth phase were collected, resuspended and seeded in the upper chamber containing serum-free culture medium at a density of 5×10^4 cells/well. Simultaneously, the medium in the lower chamber medium was refreshed or replaced with a complete culture medium supplemented with 3 mg/mL JDF and co-incubated for 24 h.

2.9. Detection of CSF-1/CSF-1R

2.9.1. Enzyme-linked immunosorbent assay (ELISA)

Cells were cultured in a normal medium or a medium containing JDF for 24 h. Then, the level of CSF-1 in the supernatant was determined using a human colony-stimulating factor ELISA kit (ml560949, mlbio, Shanghai, China). Following the instructions, the supernatants were centrifuged to remove precipitates. The samples were then added to reaction wells and incubated at 37 °C for 1 h with a biotinylated antibody. Subsequently, streptavidin-HRP conjugate was introduced to continue the incubation for an additional 30 min. The OD was measured at a wavelength of 450 nm, and the corresponding concentrations were calculated based on the established standard curve.

2.9.2. Western blot analysis

Antibodies against CSF-1 (BF0475), CSF-1R (AF0080), E-cadherin (AF0131), N-cadherin (AF5239), *p*-AKT (phosphorylated-protein kinase B; AF0016), AKT (AF6261), p-PI3K (phosphorylated-phosphatidylinositol-4,5-bisphosphate 3-kinase; AF3242), PI3K (AF6241), and cleaved-Caspase 3 (AF7022) were purchased from Affinity (Melbourne, Australia). The cells were first lysed in radioimmunoprecipitation assay (RIPA) lysis buffer (P0013, Beyotime) containing phenylmethanesulfonyl fluoride (PMSF; ST2573, Beyotime). The supernatant was collected for protein concentration detection using the bicinchoninic acid kit (BCA; P0010, Beyotime). The protein was separated on a sodium dodecyl sulfate/polyacrylamide gel and was then transferred onto a nitrocellulose membrane (66485, Pall, New York, NY, USA). These membranes were blocked with 5 % skimmed milk (A600669-0250, Sangon Biotech, Shanghai, China) for 2 h, incubated with appropriate antibodies diluted in TBST and then washed and incubated with Goat Anti-Rabbit/Mouse IgG (H + L) HRP (S0001/S0002, Affinity). The membranes were visualized using a chemiluminescence reaction after incubation, and the analysis of the optical density was determined using the Image-Pro Plus 6.0 software. GAPDH (AB0037, Abways; Shanghai, China) was used as the internal reference for comparison (AB0037, Abways, Shanghai, China).

2.9.3. Real-time quantitative PCR (qPCR)

The total RNA from the cells was extracted using the TRIzol reagent (15596026, Invitrogen), and reverse transcribed into cDNA using the HiScript III All-in-one RT SuperMix (R333-01, Vazyme, Nanjing, China). Following this, the resulting cDNA was used as the template for PCR amplification using a real-time PCR system (qTOWER3G, Analytic Jena AG, Jena, Germany), using ChamQ Universal SYBR qPCR Master Mix (Vazyme). The relative mRNA expression levels were standardized to GAPDH. The specific primers for the target genes were listed in Table 1.

2.10. Immunofluorescence

2.10.1. Tissue

Liver cancer tissue slices underwent antigen repair (EDTA antigen repair solution; G1206, Servicebio, Wuhan, China) at first. After cooling to room temperature, the tissue slices were incubated in a 3 % hydrogen peroxide solution (3032, ANNJET, Shandong, China) for 25 min to block endogenous peroxidase activity. Following that, the slices were blocked with BSA containing goat serum (C0265, Beyotime) for another 30 min. The diluted antibodies (CD206, DF4149, 1:250, Affinity; CD68, DF7518, 1:100, Affinity) were added to the slices and incubated in a humidified chamber overnight at 4 °C. The next day, corresponding secondary antibody (G1223, GB22303, Servicebio) were added, and the samples were incubated for 50 min at room temperature.

2.10.2. Cells

Cells were first clamped and fixed on slides. Then, they were permeabilized using 0.5 % Triton X-100 (X100, Amresco, Solon, USA), followed by serum blocking. These slides were incubated with CSF-1R antibody (Ab233387, Abcam) overnight at 4 °C. The following day, the slides underwent a secondary antibody reaction with HRP-conjugated secondary antibody (G1223, Servicebio).

DAPI (G1012, Servicebio) was used to restain the nucleus for 10 min. After completing the above-mentioned procedures, the samples were ultimately sealed using an antifade mounting medium (G1401, Servicebio). Image J was used to measure the number of positively-stained cells in each photograph captured using identical parameters.

2.11. Detection of apoptosis

The resuspended cells were treated with 5 μL of Annexin-V-APC and 10 μL of 7AAD staining solution (P-CA-066, Procell, Wuhan, China) for dual staining, followed by incubation for 15 min. After thorough washing with PBS, the samples were prepared for analysis. The proportion of apoptotic cells was analyzed using a FACSCanto II flow cytometer (BD Biosciences) with the CellQuest software (BD Biosciences).

2.12. Data analysis

All statistical analyses were performed using SPSS20.0 (SPSS Inc, Chicago, IL). The data were presented as the mean ± SD for at least three samples. All results were considered to be statistically significant at P-value <0.05.

3. Results

3.1. The inhibitory effect of JDF on liver cancer metastasis is related to M2 macrophages

The occurrence of liver cancer is a gradual process, leading from chronic hepatitis caused by viral infection or fatty degeneration, to liver injury, fibrosis and cirrhosis, and finally to liver cancer [29]. To determine the fundamental mechanism of action of JDF, we constructed a rat model of liver cancer and conducted resection-assisted JDF therapy. The results showed that among all rats we used, four of them experienced cancer recurrence, while eight rats developed lung metastasis (Table 2). Treatment with a high concentration of JDF did not effectively control the progression of cancer, whereas appropriate JDF treatment (low-dose groups) resulted in nearly a 50 % reduction in the proportion of metastasis compared to the metastasis reduction in the NS group (Table 2). The results of H&E staining of the rat lung tissues showed that the lung metastatic foci exhibited distinct and prominent flower-shaped clusters, with a substantial imbalance in the ratio of the tumor cell nucleus to the cytoplasm, reduction in the scant cytoplasm, indistinct cell borders, destroyed lung structures, and thickened alveolar septa (Fig. 1A). Compared to the saline group, JDF treatment inhibited the growth and progression of cancer (Fig. 1A).

The M2 macrophages were labeled using CD206 and CD68. By comparing the IF sections of the samples from the JDF treatment group and control group, we found higher levels of CD206/CD68 in the cancer tissues of the specimens with more severe metastasis (Fig. 1B, $P < 0.01$). JDF showed an inhibitory effect on M2 macrophages. These results suggested that M2 macrophages may be an important target for JDF in improving patient outcomes.

3.2. JDF inhibits the CSF-1/CSF-1R pathway of M2 macrophages

THP-1 can be induced by PMA to differentiate toward the mononuclear system, and is commonly used as a material for the formation of M2 macrophages. It was observed that THP-1 cells showed a uniformly round or quasi-round shape and grew in suspension. After M2 polarization, the cells became irregular in shape, developed extended pseudopodia and showed a clustered adherent growth

Table 1
The sequences of the specific primers for target gene.

	F	R
CSF-1	AGCCAGAAGGAGGACCAGCAAG	ACCAGCAGGTGGAAGACAGACTC
GAPDH	GTTCGTCATGGGTGTGAACC	CATCCACAGTCTTCTGGGTG

Table 2
Survival and metastasis after hepatocellular carcinoma resection in rats.

Groups	Cancer-related death	Recurrence	metastasis
Control group (n = 9)	0 (0 %)	1 (11.1 %)	2 (22.2 %)
JDF-L group (n = 8)	0 (0 %)	1 (12.5 %)	0 (0 %)
JDF-M group (n = 10)	0 (0 %)	1 (10 %)	2 (20.0 %)
JDF-H group (n = 7)	0 (0 %)	1 (14.3 %)	4 (57.1 %)

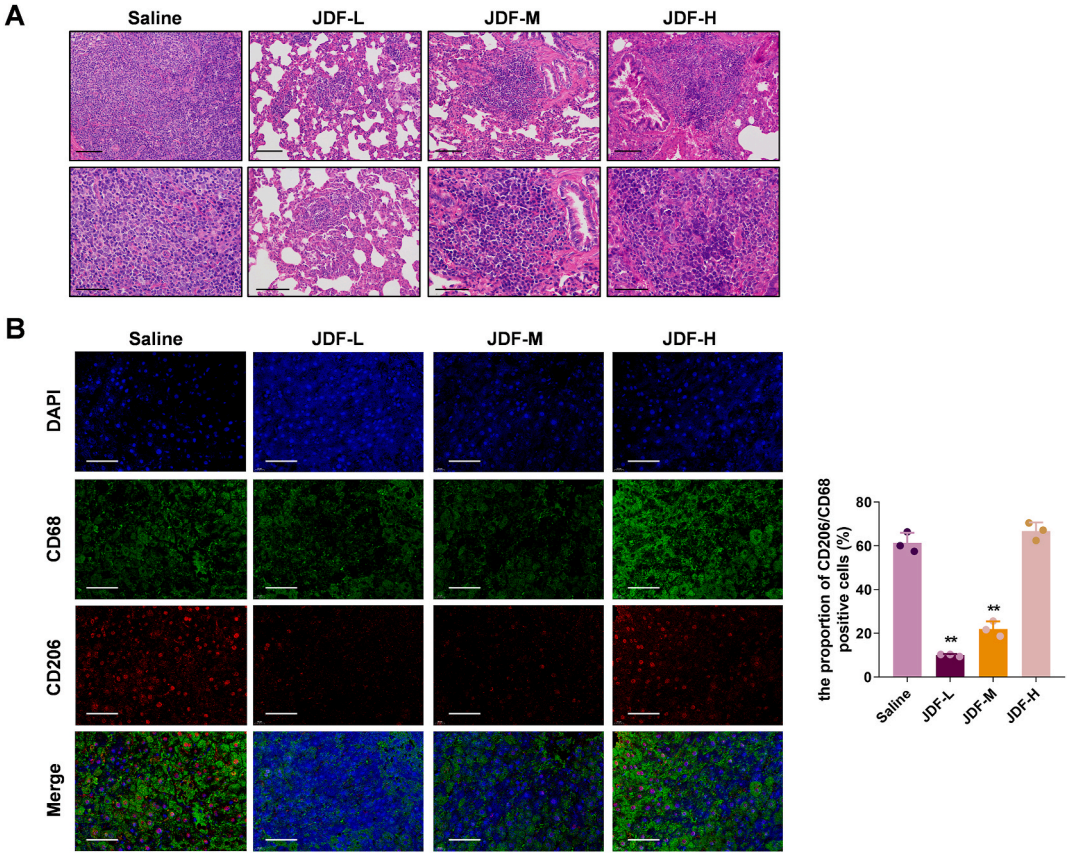

Fig. 1. Jiedu Granule formula (JDF) reduced macrophage infiltration in liver cancer, and inhibited lung metastasis. The rats were treated with JDF 3 days after resection for 2 weeks. JDF-L: 12.74 g/kg/day, JDF-M: 38.22 g/kg/day, and JDF-H: 63.7 g/kg/day. A. The results of H&E staining of lung tissue; scale bar: 200 μm; 400 μm. B. Immunofluorescence double-labeling of CD206 and CD68 in liver cancer tissue, scale bar: 130 μm; **P < 0.01 vs. Saline.

pattern (Fig. S2). Undifferentiated monocytes typically exhibit low basal levels of CD206 expression or may not express it significantly. Flow cytometry assays of CD206 confirmed the successful polarization of M2 macrophages (Fig. 2A).

Next, we conducted an investigation on the cytotoxic effects of detoxification granules JDF on M2 macrophages. The results of the MTT assay showed that JDF has the capacity to inhibit the cellular activity of M2 macrophages in a dose-dependent manner, with an IC50 of 3 mg/mL (Fig. 2B, $P < 0.01$). We also measured the levels of CSF-1 and CSF-1R in M2 macrophages, and the levels of CSF-1 in the supernatant, after treatment with different concentrations of JDF treatment. JDF treatment reduced the expressions of intracellular CSF-1 and CSF-1R proteins and also decreased the level of the CSF-1 protein in the supernatant (Fig. 2C–E, $P < 0.05$, $P < 0.01$). These findings suggested that JDF affected the CSF-1/CSF-1R pathway of M2 macrophages, which in turn inhibited the secretion of CSF-1.

3.3. JDF inhibits the migration of hepatocellular carcinoma cells

The results of the cell scratch assay showed that, compared to the control group, M2 macrophages promoted the migration of MHCC97H cells, whereas upon treatment with JDF decreased the migration ability of MHCC97H cells was reduced compared to the M2 group (Fig. 3A, $P < 0.05$). Additionally, the transwell assay yielded consistent results (Fig. 3B, $P < 0.01$). M2 macrophages probably secrete specific mediators that can affect the malignancy of MHCC97H cancer cells through paracrine signaling, and JDF, by acting on

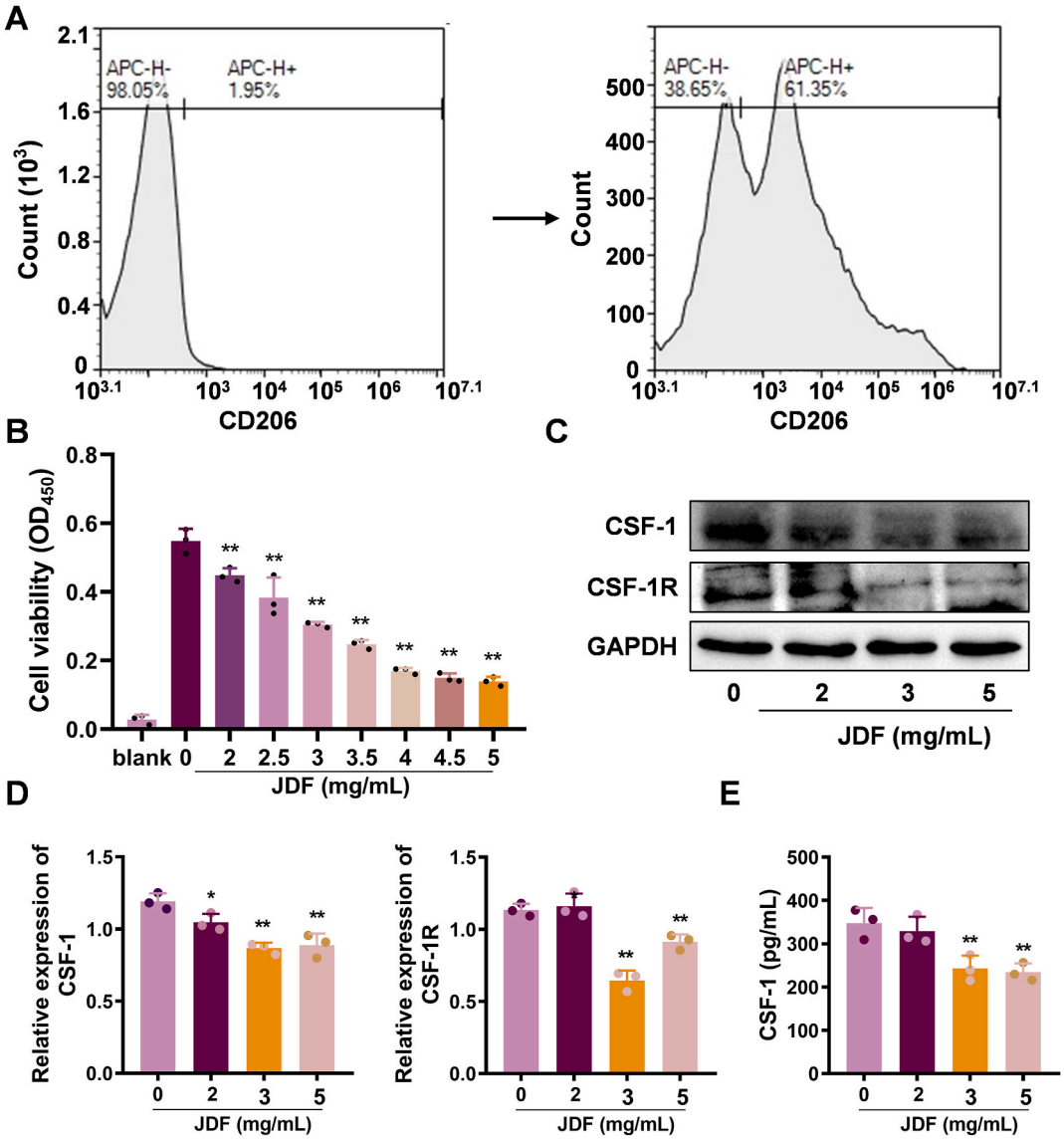

Fig. 2. JDF (3 mg/mL) decreased the level of expression of CSF-1/CSF-1R in M2 macrophages. THP-1 cells were incubated with PMA (phorbol 12-myristate 13-acetate) and IL-4 to induce differentiation into M2 macrophages. A. The M2 macrophage marker CD206 was detected by flow cytometry. M2 macrophages were treated with JDF for 24 h. B. Cell activity was assessed using the MTT assay. C-D. The protein levels of CSF-1 and CSF-1R in M2 macrophages were determined using western blotting. E. The extracellular concentration of CSF-1 produced by M2 macrophages was detected by enzyme-linked immunosorbent assay (ELISA). The original blots for the protein immunoblotting were provided in Supplementary Fig. S3. *P < 0.05 and **P < 0.01 vs. Saline.

M2 macrophages, exerts an impact on cancer cells. We found that JDF counteracted the positive effect of M2 macrophages on the migration of MHCC97H cells.

3.4. JDF decreases the level of expression of CSF-1/CSF-1R in shCSF-1-M2 macrophages

We successfully established stable transmutation of CSF-1 gene silencing using the shCSF-1 vector, as evidenced by the expression of CSF-1 (Fig. 4A–B, $P<0.01$). Subsequently, we induced shCSF-1-THP cells to become SHCSF-1-M2 macrophages (Fig. 4C, $P < 0.01$). The shCSF-1-M2 macrophages showed downregulation of the expression of CSF-1 mRNA and protein. We treated the shCSF-1-M2 macrophages with 3 mg/mL JDF for 24 h. In comparison to the supernatant of the untreated group, the supernatant of the JDF-shCSF-1 group showed a lower quantity of CSF-1 protein (Fig. 4D, $P < 0.01$). Additionally, we observed significant reduction in the expression of CSF-1 and CSF-1R (Fig. 4E, $P < 0.05$, $P < 0.01$). JDF could further decrease the expression of CSF-1 when the concentration of CSF-1 was low.

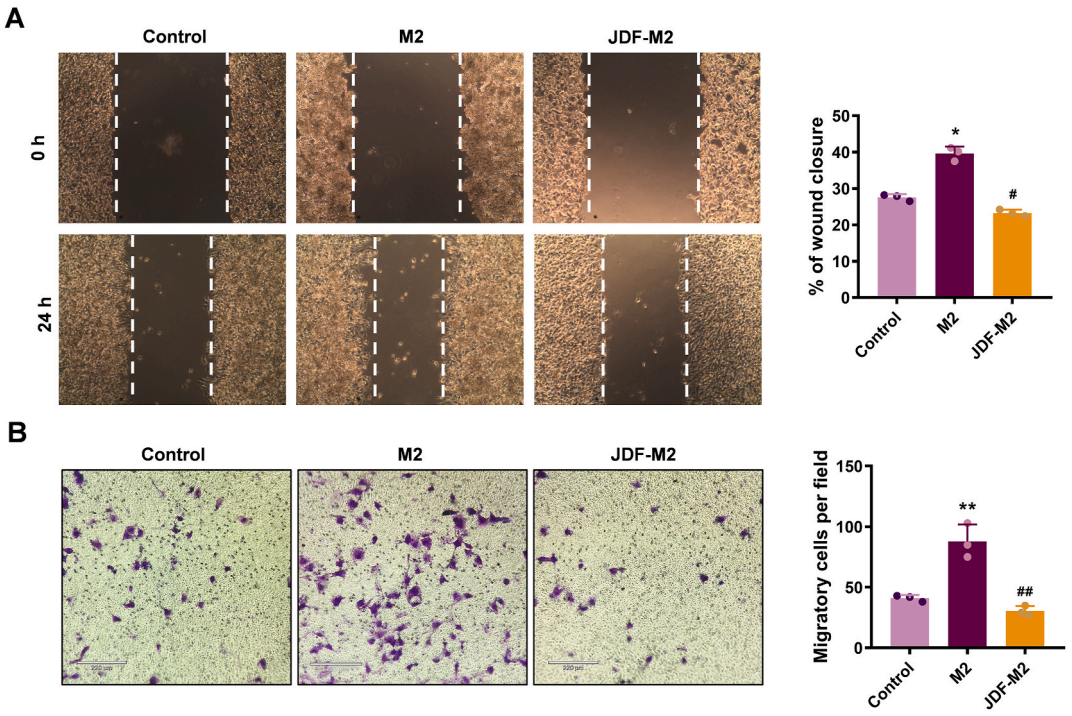

Fig. 3. The conditioned medium (CM) of JDF-M2 inhibited MHCC97H cell migration. A. A cell scratch assay was used to measure the migration ability of MHCC97H cancer cells. B. Transwell assay was used to measure the migration ability of MHCC97H cancer cells. **P < 0.01 vs. Control, ##P < 0.01 vs. M2.

3.5. JDF inhibits the migration capability of liver cancer cells through CSF-1

The above experiments demonstrated that JDF has an impact on the CSF-1/CSF-1R pathway of M2 macrophages. We speculated whether CSF-1 can act as a target for JDF therapy. Based on experiments, we found that in the shCSF-1 group and the JDF group, delayed wound recovery occurred in the scratch area of MHCC97H cells, and fewer migrated cells were present in the transwell lower chamber (Fig. 5A–B, $P<0.01$). Compared to ShCSF-1 group, JDF-ShCSF-1 group had a stronger inhibitory effect on the migration ability of MHCC97H cells (Fig. 5A–B, $P < 0.05$). The results of the cell scratch assay and transwell assays collectively suggested that CSF-1 might be the key mediator between M2 macrophages and MHCC97H cells. Treatment with JDF can downregulate CSF-1 levels in M2 macrophages, thereby inhibiting the migration of MHCC97H cells.

Next, we conducted cell co-culture experiments. As expected, the number of migrated MHCC-97H cells was significantly reduced in the JDF, ShCSF-1, and JDF-ShCSF-1 groups compared to that in the Scramble group; the cells in the JDF-ShCSF-1 group experienced the most prominent effect (Fig. 6A, $P < 0.05$, $P < 0.01$). Western blotting showed that knockdown of endogenous CSF-1, or treatment with JDF, significantly enhanced the expression of E-cadherin while concurrently suppressing the expression of N-cadherin protein (Fig. 6B, $P < 0.05$, $P < 0.01$). The CSF-1/CSF-1R signaling pathway of M2 macrophages was significantly inhibited after CSF-1 was knocked down and/or after subsequent treatment with JDF (Fig. 6C–E, $P < 0.05$, $P < 0.01$). Compared to the Scramble group, the M2 macrophages in the JDF, ShCSF-1, and JDF-ShCSF-1 groups exhibited a decrease in the CSF-1 mRNA levels, a reduction in the number of $CSF\text{-}1R^{+}$ cells, and a decrease in the CSF-1 protein levels in the supernatant. These pieces of evidence revealed that JDF treatment can suppress the motor ability of liver cancer by regulating the CSF-1/CSF-1R signaling pathway in M2 macrophages.

3.6. JDF inhibits the CSF-1/PI3K/AKT signaling pathway and promotes apoptosis of M2 macrophages

Treatment with JDF or knockdown of CSF-1 alone decreased the phosphorylation levels of PI3K and AKT in M2 macrophages (Fig. 7A, $P < 0.01$). Suppression of the PI3K/AKT pathway was more pronounced in shCSF-1 M2 macrophages treated with JDF, compared to the JDF and shCSF-1 groups (Fig. 7A, $P < 0.05$, $P < 0.01$). After treatment with the 740Y–P agonist, phosphorylation levels of PI3K and AKT increased (Fig. 7A, $P < 0.05$, $P < 0.01$). The changes in the PI3K/AKT signaling pathway were consistent with the apoptotic changes in M2 macrophages (Fig. 7B–C, $P < 0.01$). Additionally, treatment with JDF or knockdown of CSF-1 promoted the expression of cleaved caspase-3 (Fig. 7D, $P < 0.01$). Following treatment with JDF, the expression of cleaved caspase-3 (17 kDa) was found to be minimized in shCSF-1M2 macrophages, an effect that was notably reversed after administration of the 740Y–P agonist (Fig. 7B–D, $P < 0.01$). JDF promoted the apoptosis of M2 macrophages by inhibiting the CSF-1/PI3K/AKT signaling pathway, which lead to the activation of caspase-3.

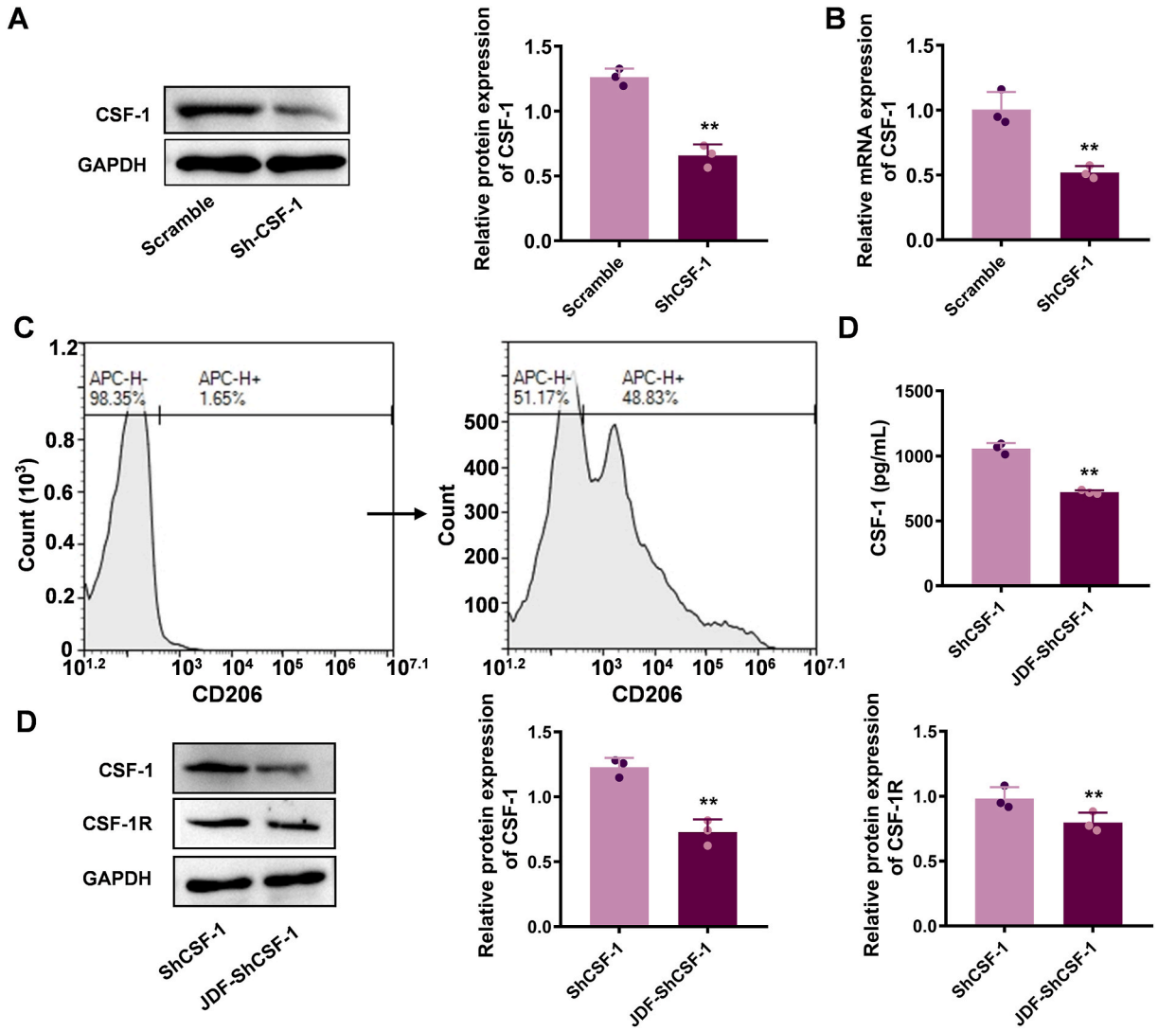

Fig. 4. Treatment with JDF (3 mg/mL) and knocking down of shCSF-1 decreased the level of expression of CSF-1/CSF-1R in M2 macrophages. The shCSF-1 lentivirus was transfected. A. qPCR was used to determine the transcription level of CSF-1. B. Western blotting was used to determine the level of CSF-1 protein. C. The M2 macrophage marker CD206 was detected by flow cytometry. D. The extracellular CSF-1 concentration was determined by ELISA. E. Western blotting was used to determine the expression of CSF-1 and CSF-1R proteins after treatment with JDF. The original blots for the protein immunoblotting were provided in Supplementary Fig. S4. **P < 0.01 vs. Scramble, ##P < 0.01 vs. shCSF-1.

4. Discussion

Several studies have demonstrated that patients suffering from lung cancer can benefit from Traditional Chinese Medicine treatment across overall stages of the disease [30,31]. JDF is a commonly used Chinese herbal medicine formula. As an alternative or an adjuvant treatment, JDF has been found to prolong the survival of patients, and reduce the risk of postoperative recurrence and metastasis in several clinical studies, including those on JDF treatment combined with cinobufacini injection [32], JDF treatment combined with TACE therapy (unresectable liver cancer) [33,34], and postoperative treatment with JDF [16]. A previous study demonstrated that JDF inhibits epithelial-mesenchymal transition (EMT) in liver cancer cells via the Smad2/3 signaling pathways, thereby suppressing cell migration and invasion [35]. Our findings supported the beneficial effect of JDF in preventing lung metastasis after liver cancer surgery. Additionally, our study revealed that JDF can regulate the tumor immune microenvironment, which contributes to the cross-talk between liver cancer cells and macrophages.

The complex interactions between cancer cells and stromal cells ultimately create a microenvironment that strongly favors the survival and potential spread of tumor cells [36]. In the early stages of cancer, M1 macrophages dominate and activate tumor immunity. However, as the tumor progresses, M2 macrophages become the dominant type of infiltrating cells in the microenvironment. Even after surgical removal, the TME persists, consequently influencing the prognosis of patients [37]. The results of the

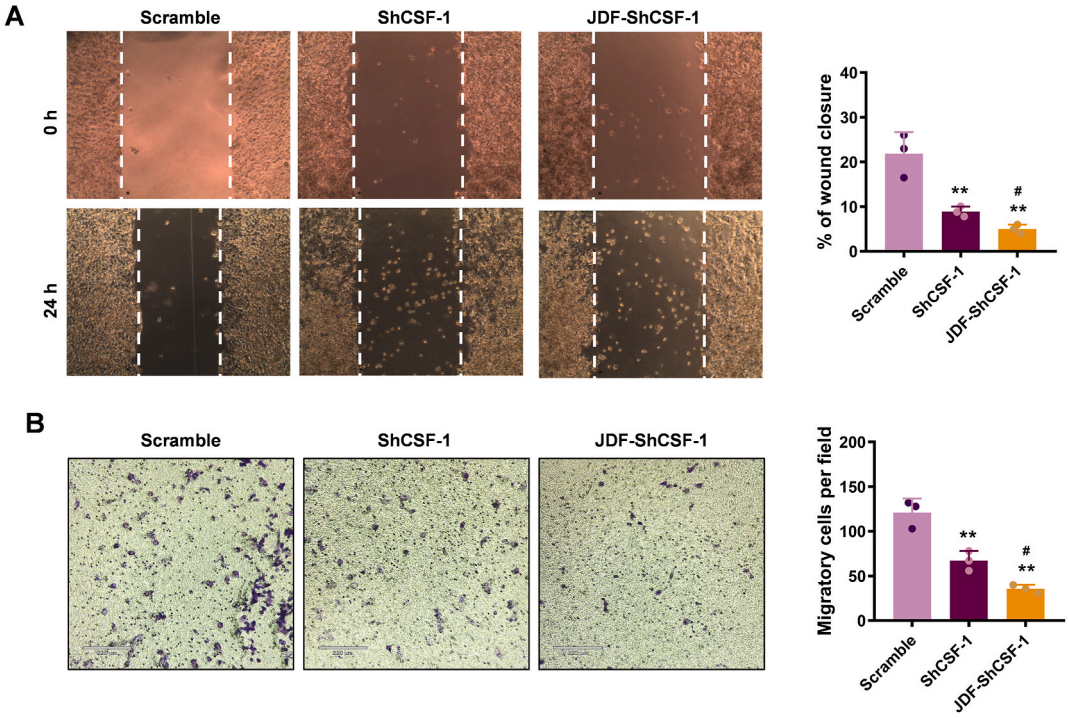

Fig. 5. JDF-CM and shCSF-1-CM inhibited the migration of MHCC97H cells. A. Cell scratch assay was used to measure the migration ability of MHCC97H cancer cells. B. Transwell assay was used to measure the migration ability of MHCC97H cancer cells. $^{**}P < 0.01$ vs. Scramble, $^{\#}P < 0.05$ vs. shCSF-1.

immunofluorescence assays indicated that JDF inhibited the infiltration of M2 macrophages. JDF can affect the motor capacity of liver cancer cells by modulating the immune response and the local microenvironment. Accumulated data have demonstrated that M2 macrophages promote cancer recurrence and metastasis through multiple pathways, including: promoting cancer stem cell properties [21,38], inducing angiogenesis (via vascular endothelial growth factor, interleukin-1β, tumor necrosis factor-α) [39], facilitating matrix degradation (via matrix metalloproteinases) [40], triggering EMT [41], and suppressing the immune response (via interleukin-10, and transforming growth factor-β) [42]. In this study, when M2 macrophages treated with JDF were co-cultured with cancer cells, a marked inhibition of migration and EMT was observed in MHCC-97H cells. What's more, the invasion of tumor cells into the interstitial tissue is a crucial step in the establishment of metastasis. Some researchers have found that macrophages and tumors co-migrate and rely on each other [43]. Therefore, the inhibition of M2 macrophages infiltration seems to be one of the key mechanisms for JDF to inhibit the metastasis of liver cancer cells.

The cytokine CSF-1 regulates macrophage activity and plays a crucial role in the proliferation, differentiation, and survival of macrophages [44]. CSF-1R is the only identified and specific receptor for CSF-1. The binding of ligands to CSF1R is considered to induce receptor dimerization, intermolecular autophosphorylation of CSF-1, and activation of the kinase domain [45]. In this study, it was found that JDF decreased the levels of CSF-1 and CSF-1R in M2 macrophages. Activated macrophages undergo morphological changes, accompanied by the spreading of thin membranes on the cell surface, followed by an increase in cell polarization and movement [46]. Thus, besides inhibiting macrophage survival, JDF may also influence the recruitment and polarization of macrophages by regulating the CSF-1/CSF-1R pathway. Furthermore, Yang et al. found that the discovered supply of CSF-1 is much lower than its consumption by macrophages, suggesting that IL-6-driven generation of M2 macrophages largely depends on the autocrine consumption of CSF-1 [47]. The regulation of endogenous CSF1 potentially serve as a crucial factor in the activity of M2 macrophages. In addition, macrophage populations also respond to chemokine levels in TME, including CSF-1, interferon (IFN)-γ, CC and CXC chemokines [48,49]. Relevant studies have shown that JDF can inhibit CXCL1/2/3 chemokines in liver cancer tissue. CXCL-1 can recruit macrophages into the TME [50]. JDF may also impact the activity and function of macrophages by altering the composition of the TME.

The paracrine CSF-1/CSF-1R signaling loop can also selectively exert its effects on tumors progression [51]. Cancer cells can express the CSF-1R receptor, and upon binding of the receptor with CSF-1, it induces morphological changes in tumor cells, facilitates the dissociation of the adhesion molecule E-cadherin from cytoskeletal proteins, releases connections between tumor cell complexes, disrupts cell adhesion, and reduces the ability of tumor cells to adhere to the surface of other tumor cells, thereby promoting the ability of tumor cells to leave the primary site through movement and proliferation [51,52]. Our ELISA results showed a reduction in the content of CSF-1 in the supernatant of M2 macrophages after treatment with JDF. This reduction is potentially suggestive of the mechanism responsible for the inhibition of cancer cell migration, although additional evidence is required to support this speculation.

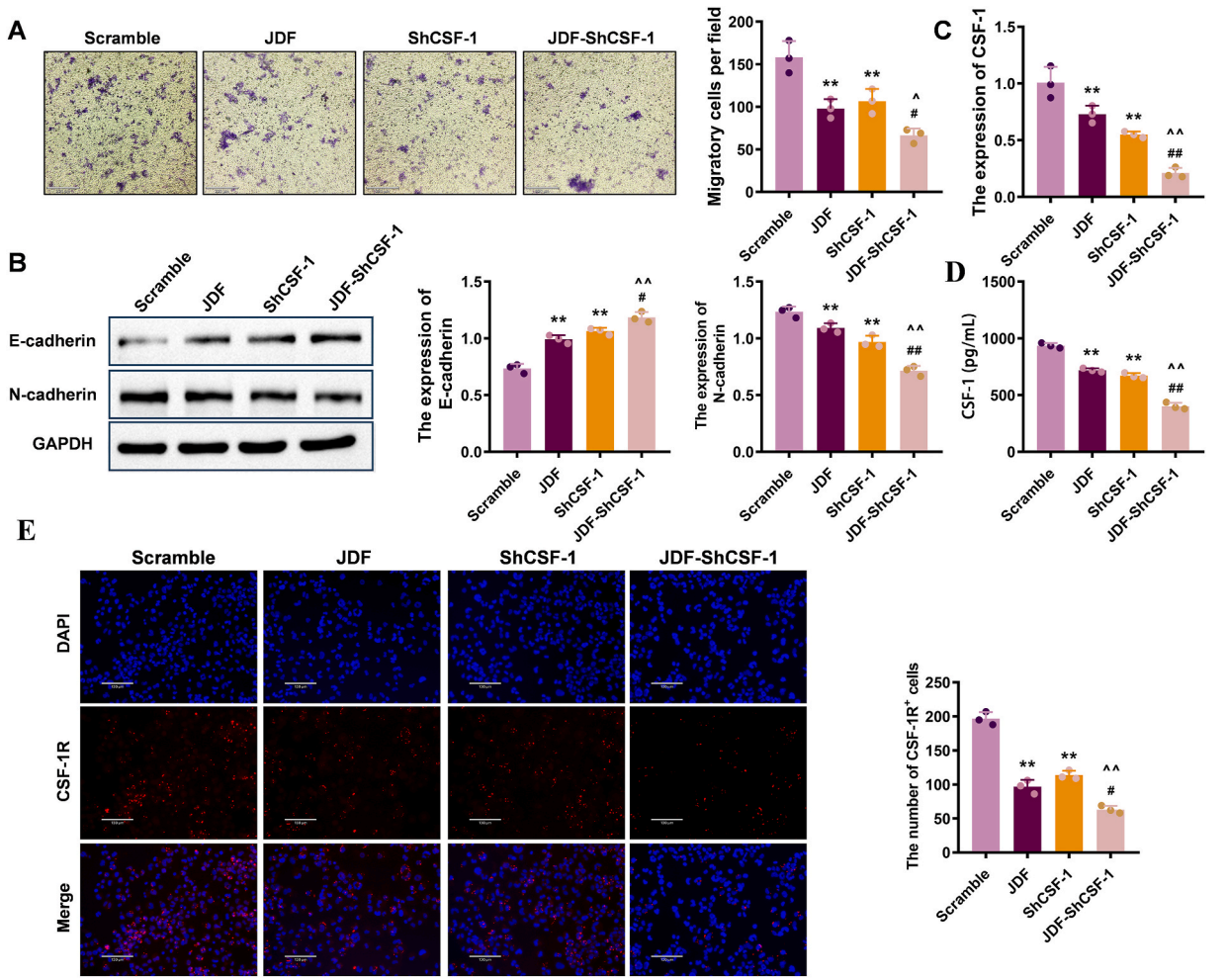

Fig. 6. Treatment with JDF (3 mg/mL) reduced the migration of MHCC97H cells when co-cultured with M2 macrophages by knocking down CSF-1. A. Transwell assay was used to measure the migration ability of MHCC97H cancer cells. B. Western blotting was used to determine the expression of CSF-1 protein in MHCC-97H cells. C. qPCR detected the expression of CSF-1 mRNA in M2 macrophages. D. The concentration of CSF-1 in the lower chamber culture system was determined by ELISA. E. Immunofluorescence detection of CSF-1R^{+} M2 macrophages. The original blots for the protein immunoblotting were provided in Supplementary Fig. S5. **P < 0.01 vs. Scramble; $^{\#}$P < 0.05 and $^{\#\#}$P < 0.01 vs. shCSF-1; $^{\wedge}$P < 0.05 and $^{\wedge\wedge}$P < 0.01 vs. JDF.

Interestingly, N-Sumanta Goswami et al. found that treatment with CSF-1-CM alone did not enhance the migration of cancer cells, but rather the positive circuits between tumor cells secreting CSF-1 and macrophages producing EGF regulated the morphology of these cells [53]. What's more, CSF-1 induced M2 macrophages showed high levels of expression of IL-12/23, along with the expression of CCL17, CCL22, and IL-10 [54,55]. The impact of JDF crosstalk signals on macrophages and liver cancer cells still requires further elucidation, such as miR-501-3p [56], and the plasminogen activator inhibitor-1 pathway [57].

The PI3K/Akt signaling pathway is associated with phosphatidylinositol and strongly influences cell survival [58]. Our findings suggested that JDF can promote apoptosis of M2 macrophages by inhibiting the CSF-1/PI3K/AKT signaling pathway. Previous studies have revealed that the PI3K/AKT signaling pathway inhibits apoptosis by impeding the initiation of apoptosis, such as the activation of caspase-9, thereby blocking caspase-3 activation [59]. JDF promotes the cleavage and activation of downstream pro-caspase-3 by inhibiting the signaling pathway. Additionally, studies on mice lacking individual Akt or PI3K subtypes, and the use of RNA interference techniques, have found that different components of the Akt signaling pathway play distinct roles in macrophage biology and the regulation of inflammatory diseases [60]. The PI3K/AKT/mTOR pathway is also involved in mediating autophagy [61], the release of inflammatory cytokines [62], and the phagocytosis and metabolism of macrophages [63].

In summarize, we investigated the possible mechanisms by which JDF decreases liver cancer metastasis. For a more compelling substantiation of our findings, supplementary evidence from *in vivo* studies utilizing advanced imaging techniques, such as PET-CT, would be advantageous. Our findings showed that JDF can effectively reduce M2 macrophage infiltration. It can also regulate the survival of M2 macrophages through CSF1/PI3K/Akt signaling; thus, it can play a role in inhibiting EMT and migration of cancer cells. These results provide a new perspective for the clinical application of JDF. However, given the variability of macrophages and the

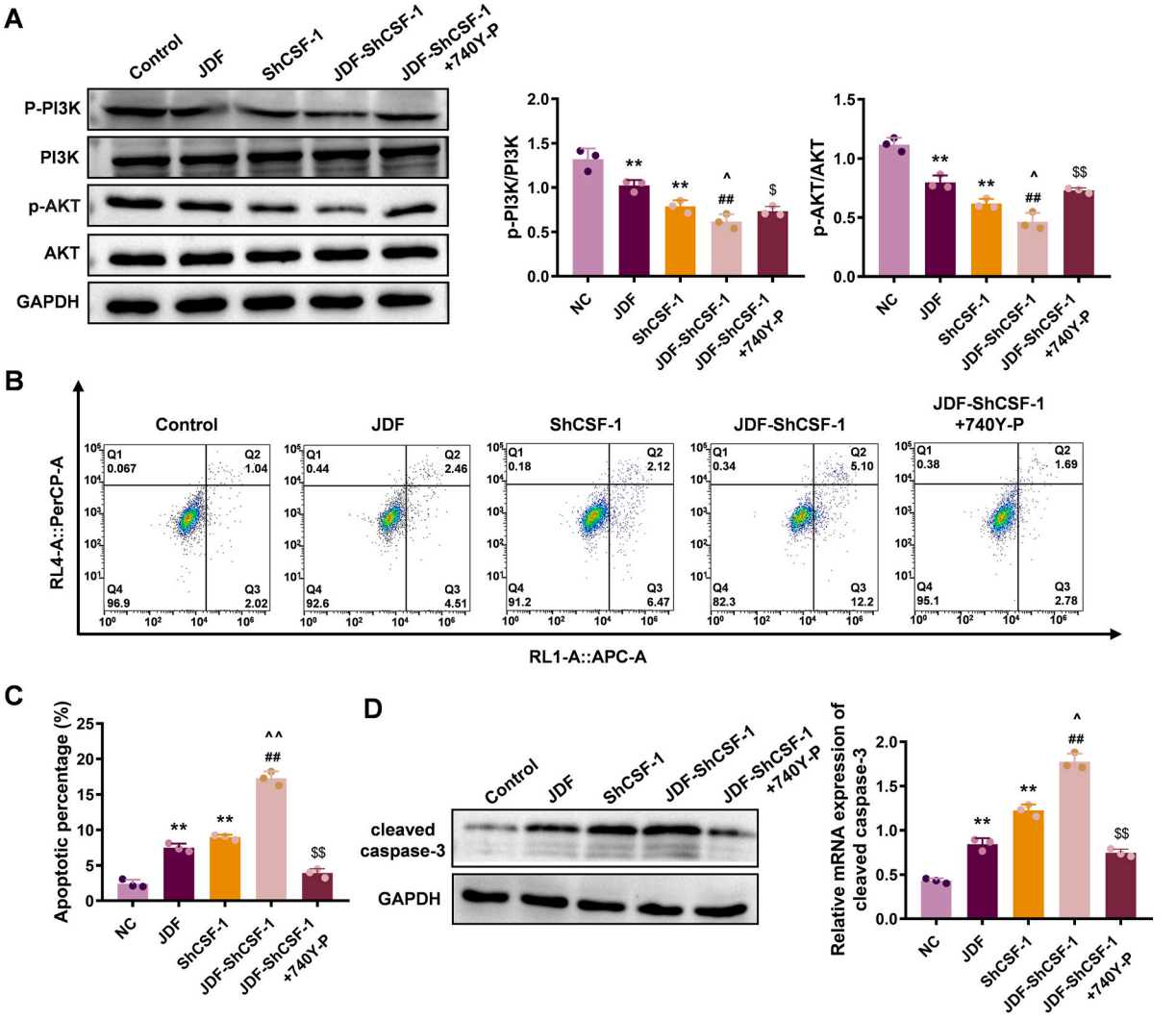

Fig. 7. Treatment with JDF (3 mg/mL) inhibited the CSF-1/PI3K/AKT signaling pathway and promoted apoptosis of M2 macrophages. A. Western blotting was used to determine the activity of PI3K/AKT pathway. B–C. The apoptosis of M2 macrophages was measured by flow cytometry. D. Western blotting was used to determine the expression of cleaved caspase-3. The original blots for the protein immunoblotting were provided in Supplementary Fig. S6. **P < 0.01 vs. Scramble; #P < 0.05 and ##P < 0.01 vs. shCSF-1; ^ P < 0.05 vs. JDF; $ P < 0.05 and $$ P < 0.01 vs. JDF-shCSF-1.

limitations of the conditions in this study, further studies are needed to solidify our results.

Funding

This study was supported by National Natural Science Foundation of China (Nos.: 81904157 and 82304932), Training Program for High-caliber Talents of Clinical Research at Affiliated Hospitals of SHUTCM (No.: TCM[2022]14), Shanghai University of TCM Excellent Talents Training Program (No.: TCM[2020]10), Research project of Shanghai Municipal Health Commission (No.: 202340139) and Traditional Chinese Medicine Research Project of Shanghai Municipal Health Commission (No.: 2022QN051).

Data availability

Data will be made available on request.

Ethics statement

All experiments were approved by the Ethics Committee of experimental animal medicine of Shanghai Hospital of Traditional

Chinese Medicine (Approval No.: 2020002).

CRediT authorship contribution statement

Xiaolin Liu: Writing – original draft, Software, Resources, Methodology, Formal analysis, Data curation. **Zongyao Wang:** Writing – review & editing, Software, Resources, Methodology, Formal analysis, Data curation. **Xiang Lv:** Writing – review & editing, Visualization, Software, Resources, Formal analysis. **Zhihui Tao:** Writing – review & editing, Visualization, Software, Resources, Formal analysis. **Liubing Lin:** Writing – review & editing, Visualization, Software, Resources, Methodology, Formal analysis. **Shasha Zhao:** Writing – review & editing, Software, Resources, Methodology, Data curation. **Kehui Zhang:** Writing – review & editing, Visualization, Software, Methodology. **Yong Li:** Writing – review & editing, Validation, Supervision, Project administration, Investigation, Funding acquisition, Conceptualization.

Declaration of competing interest

The authors declare that they have no known competing financial interests or personal relationships that could have appeared to influence the work reported in this paper.

Acknowledgments

The language of this study was professionally edited by ExEditing.com.

Appendix A. Supplementary data

Supplementary data to this article can be found online at https://doi.org/10.1016/j.heliyon.2024.e34968.

References

[1] F. Bray, M. Laversanne, H. Sung, J. Ferlay, R.L. Siegel, I. Soerjomataram, et al., Global cancer statistics 2022: GLOBOCAN estimates of incidence and mortality worldwide for 36 cancers in 185 countries, CA A Cancer J. Clin. 74 (3) (2024) 229–263, https://doi.org/10.3322/caac.21834.
[2] R.L. Siegel, K.D. Miller, A. Jemal, Cancer statistics, 2020, CA A Cancer J. Clin. 70 (1) (2020) 7–30, https://doi.org/10.3322/caac.21590.
[3] K. Feng, J. Yan, X. Li, F. Xia, K. Ma, S. Wang, et al., A randomized controlled trial of radiofrequency ablation and surgical resection in the treatment of small hepatocellular carcinoma, J. Hepatol. 57 (4) (2012) 794–802, https://doi.org/10.1016/j.jhep.2012.05.007.
[4] X.L. Xu, X.D. Liu, M. Liang, B.M. Luo, Radiofrequency ablation versus hepatic resection for small hepatocellular carcinoma: systematic review of randomized controlled trials with meta-analysis and trial sequential analysis, Radiology 287 (2) (2018) 461–472, https://doi.org/10.1148/radiol.2017162756.
[5] Y. Peng, F. Liu, Y. Wei, B. Li, Outcomes of laparoscopic repeat liver resection for recurrent liver cancer: a system review and meta-analysis, Medicine (Baltim.) 98 (41) (2019) e17533, https://doi.org/10.1097/MD.0000000000017533.
[6] Z.C. Jin, Q. Zhang, H.D. Zhu, G.J. Teng, [Research progress of adjuvant TACE therapy for liver cancer after radical resection], Zhonghua Gan Zang Bing Za Zhi 30 (3) (2022) 340–344, https://doi.org/10.3760/cma.j.cn501113-20200609-00302.
[7] J. Wu, Z. Yin, L. Cao, X. Xu, T. Yan, C. Liu, et al., Adjuvant pegylated interferon therapy improves the survival outcomes in patients with hepatitis-related hepatocellular carcinoma after curative treatment: a meta-analysis, Medicine (Baltim.) 97 (28) (2018) e11295, https://doi.org/10.1097/MD.0000000000011295.
[8] K. Takeda, Y. Kikuchi, Y.U. Sawada, T. Kumamoto, J. Watanabe, C. Kuniski, et al., Efficacy of adjuvant chemotherapy following curative resection of colorectal cancer liver metastases, Anticancer Res. 42 (11) (2022) 5497–5505, https://doi.org/10.21873/anticanres.16055.
[9] K. Li, K. Xiao, S. Zhu, Y. Wang, W. Wang, Chinese herbal medicine for primary liver cancer therapy: perspectives and challenges, Front. Pharmacol. 13 (2022) 889799, https://doi.org/10.3389/fphar.2022.889799.
[10] X.F. Zhai, C.X. Qiao, Q. Liu, Z. Chen, C.Q. Ling, Quality assessment of clinical research on liver cancer treated by intra-arterial infusion of Chinese medicine, Chin. J. Integr. Med. 20 (11) (2014) 870–875, https://doi.org/10.1007/s11655-013-1555-y.
[11] Y. Fan, Z. Ma, L. Zhao, W. Wang, M. Gao, X. Jia, et al., Anti-tumor activities and mechanisms of Traditional Chinese medicines formulas: a review, Biomed. Pharmacother. 132 (2020) 110820, https://doi.org/10.1016/j.biopha.2020.110820.
[12] D. Zeng, X.X. Li, Y.X. Bian, L.B. Liu, X.Y. Liang, 山慈菇含药血清对SMMC-7721细胞侵袭、黏附能力的影响, vol. 30, Journal of the Fourth Military Medical University, 2009, p. 4.
[13] J.S. Shim, J.H. Kim, J. Lee, S.N. Kim, H.J. Kwon, Anti-angiogenic activity of a homoisoflavanone from Cremastra appendiculata, Planta Med. 70 (2) (2004) 171–173, https://doi.org/10.1055/s-2004-815496.
[14] T. Fang, J. Hou, M. He, L. Wang, M. Zheng, X. Wang, et al., Actinidia chinensis Planch root extract (acRoots) inhibits hepatocellular carcinoma progression by inhibiting EP3 expression, Cell Biol. Toxicol. 32 (6) (2016) 499–511, https://doi.org/10.1007/s10565-016-9351-z.
[15] Q.P. Zhu, G.Q. Xie, X.D. Guo, M. Zx, Q. Hk, W. Gu, et al., Clearing away heat and toxic materials formula combined with Western medicine's conventional therapy for the prevention and treatment of mid-late stage primary liver cancer after transcatheter arterial chemoembolization-induced syndrome: a clinical study, Shanghai Traditional Chinese Medicine Journal 46 (2012) 35.
[16] X.F. Zhai, X.L. Liu, F. Shen, J. Fan, C.Q. Ling, Traditional herbal medicine prevents postoperative recurrence of small hepatocellular carcinoma: a randomized controlled study, Cancer 124 (10) (2018) 2161–2168, https://doi.org/10.1002/cncr.30915.
[17] X.F. Zhai, Z. Chen, B. Li, F. Shen, J. Fan, W.P. Zhou, et al., Traditional herbal medicine in preventing recurrence after resection of small hepatocellular carcinoma: a multicenter randomized controlled trial, J Integr Med 11 (2) (2013) 90–100, https://doi.org/10.3736/jintegrmed2013021.
[18] K. Cheng, N. Cai, J. Zhu, X. Yang, H. Liang, W. Zhang, Tumor-associated macrophages in liver cancer: from mechanisms to therapy, Cancer Commun. 42 (11) (2022) 1112–1140, https://doi.org/10.1002/cac2.12345.
[19] M. Locati, G. Curtale, A. Mantovani, Diversity, mechanisms, and significance of macrophage plasticity, Annu. Rev. Pathol. 15 (2020) 123–147, https://doi.org/10.1146/annurev-pathmechdis-012418-012718.
[20] S. Qiu, L. Xie, C. Lu, C. Gu, Y. Xia, J. Lv, et al., Gastric cancer-derived exosomal miR-519a-3p promotes liver metastasis by inducing intrahepatic M2-like macrophage-mediated angiogenesis, J. Exp. Clin. Cancer Res. 41 (1) (2022) 296, https://doi.org/10.1186/s13046-022-02499-8.

[21] O.W. Yeung, C.M. Lo, C.C. Ling, X. Qi, W. Geng, C.X. Li, et al., Alternatively activated (M2) macrophages promote tumour growth and invasiveness in hepatocellular carcinoma, J. Hepatol. 62 (3) (2015) 607–616, https://doi.org/10.1016/j.jhep.2014.10.029.

[22] A. Mantovani, F. Marchesi, A. Malesci, L. Laghi, P. Allavena, Tumour-associated macrophages as treatment targets in oncology, Nat. Rev. Clin. Oncol. 14 (7) (2017) 399–416, https://doi.org/10.1038/nrclinonc.2016.217.

[23] Y. Xiong, D. Song, Y. Cai, W. Yu, Y.G. Yeung, E.R. Stanley, A CSF-1 receptor phosphotyrosine 559 signaling pathway regulates receptor ubiquitination and tyrosine phosphorylation, J. Biol. Chem. 286 (2) (2011) 952–960, https://doi.org/10.1074/jbc.M110.166702.

[24] I. Espinosa, A.H. Beck, C.H. Lee, S. Zhu, K.D. Montgomery, R.J. Marinelli, et al., Coordinate expression of colony-stimulating factor-1 and colony-stimulating factor-1-related proteins is associated with poor prognosis in gynecological and nongynecological leiomyosarcoma, Am. J. Pathol. 174 (6) (2009) 2347–2356, https://doi.org/10.2353/ajpath.2009.081037.

[25] A. Budhu, M. Forgues, Q.H. Ye, H.L. Jia, P. He, K.A. Zanetti, et al., Prediction of venous metastases, recurrence, and prognosis in hepatocellular carcinoma based on a unique immune response signature of the liver microenvironment, Cancer Cell 10 (2) (2006) 99–111, https://doi.org/10.1016/j.ccr.2006.06.016.

[26] A. Ahmad, R. Ahmad, Resveratrol mitigate structural changes and hepatic stellate cell activation in N'-nitrosodimethylamine-induced liver fibrosis via restraining oxidative damage, Chem. Biol. Interact. 221 (2014) 1–12, https://doi.org/10.1016/j.cbi.2014.07.007.

[27] F. Piccioni, M. Malvicini, M.G. Garcia, A. Rodriguez, C. Atorrasagasti, N. Kippes, et al., Antitumor effects of hyaluronic acid inhibitor 4-methylumbelliferone in an orthotopic hepatocellular carcinoma model in mice, Glycobiology 22 (3) (2012) 400–410, https://doi.org/10.1093/glycob/cwr158.

[28] W. Chanput, J.J. Mes, H.F. Savelkoul, H.J. Wichers, Characterization of polarized THP-1 macrophages and polarizing ability of LPS and food compounds, Food Funct. 4 (2) (2013) 266–276, https://doi.org/10.1039/c2fo30156c.

[29] V.W. Yuen, C.C. Wong, Hypoxia-inducible factors and innate immunity in liver cancer, J. Clin. Invest. 130 (10) (2020) 5052–5062, https://doi.org/10.1172/JCI137553.

[30] W. Bochuan, Z. Yong, Z. Qiuyun, Z. Zhiqiang, L. Changyong, W. Zhendong, et al., Reveal the mechanisms of prescriptions for liver cancer' treatment based on two illustrious senior TCM physicians, J. Tradit. Chin. Med. 43 (1) (2023) 188–197, https://doi.org/10.19852/j.cnki.jtcm.20221013.001.

[31] J. Zhou, H. Sun, Z. Wang, W. Cong, J. Wang, M. Zeng, et al., Guidelines for the diagnosis and treatment of hepatocellular carcinoma (2019 edition), Liver Cancer 9 (6) (2020) 682–720, https://doi.org/10.1159/000509424.

[32] Z. Chen, H.Y. Chen, Q.B. Lang, B. Li, X.F. Zhai, Y.Y. Guo, et al., Preventive effects of jiedu granules combined with cinobufacini injection versus transcatheter arterial chemoembolization in post-surgical patients with hepatocellular carcinoma: a case-control trial, Chin. J. Integr. Med. 18 (5) (2012) 339–344, https://doi.org/10.1007/s11655-012-1083-1.

[33] Y. Yu, Q. Lang, Z. Chen, B. Li, C. Yu, D. Zhu, et al., The efficacy for unresectable hepatocellular carcinoma may be improved by transcatheter arterial chemoembolization in combination with a traditional Chinese herbal medicine formula: a retrospective study, Cancer 115 (22) (2009) 5132–5138, https://doi.org/10.1002/cncr.24567.

[34] H. Zhao, X. Zhai, Z. Chen, X. Wan, L. Chen, F. Shen, et al., Transarterial chemoembolization combined with Jie-du granule preparation improves the survival outcomes of patients with unresectable hepatocellular carcinoma, Oncotarget 8 (28) (2017) 45234–45241, https://doi.org/10.18632/oncotarget.16804.

[35] S. Liang, Y. Zou, J. Gao, X. Liu, W. Lin, Z. Yin, et al., The Chinese medicine, jiedu recipe, inhibits the epithelial mesenchymal transition of hepatocellular carcinoma via the regulation of smad2/3 dependent and independent pathways, Evid Based Complement Alternat Med 2018 (2018) 5629304, https://doi.org/10.1155/2018/5629304.

[36] F. Mirshahi, H.F. Aqbi, M. Isbell, S.H. Manjili, C. Guo, M. Saneshaw, et al., Distinct hepatic immunological patterns are associated with the progression or inhibition of hepatocellular carcinoma, Cell Rep. 38 (9) (2022) 110454, https://doi.org/10.1016/j.celrep.2022.110454.

[37] E. Cariani, M. Pilli, A. Zerbini, C. Rota, A. Olivani, G. Pelosi, et al., Immunological and molecular correlates of disease recurrence after liver resection for hepatocellular carcinoma, PLoS One 7 (3) (2012) e32493, https://doi.org/10.1371/journal.pone.0032493.

[38] W. Li, X. Xin, X. Li, J. Geng, Y. Sun, Exosomes secreted by M2 macrophages promote cancer stemness of hepatocellular carcinoma via the miR-27a-3p/TXNIP pathways, Int. Immunopharm. 101 (Pt A) (2021) 107585, https://doi.org/10.1016/j.intimp.2021.107585.

[39] B.Z. Qian, J.W. Pollard, Macrophage diversity enhances tumor progression and metastasis, Cell 141 (1) (2010) 39–51, https://doi.org/10.1016/j.cell.2010.03.014.

[40] K. Vinnakota, Y. Zhang, B.C. Selvanesan, G. Topi, T. Salim, J. Sand-Dejmek, et al., M2-like macrophages induce colon cancer cell invasion via matrix metalloproteinases, J. Cell. Physiol. 232 (12) (2017) 3468–3480, https://doi.org/10.1002/jcp.25808.

[41] W. Li, X. Zhang, F. Wu, Y. Zhou, Z. Bao, H. Li, et al., Gastric cancer-derived mesenchymal stromal cells trigger M2 macrophage polarization that promotes metastasis and EMT in gastric cancer, Cell Death Dis. 10 (12) (2019) 918, https://doi.org/10.1038/s41419-019-2131-y.

[42] Y. Chen, Y. Song, W. Du, L. Gong, H. Chang, Z. Zou, Tumor-associated macrophages: an accomplice in solid tumor progression, J. Biomed. Sci. 26 (1) (2019) 78, https://doi.org/10.1186/s12929-019-0568-z.

[43] J. Wyckoff, W. Wang, E.Y. Lin, Y. Wang, F. Pixley, E.R. Stanley, et al., A paracrine loop between tumor cells and macrophages is required for tumor cell migration in mammary tumors, Cancer Res. 64 (19) (2004) 7022–7029, https://doi.org/10.1158/0008-5472.CAN-04-1449.

[44] F.J. Pixley, E.R. Stanley, CSF-1 regulation of the wandering macrophage: complexity in action, Trends Cell Biol. 14 (11) (2004) 628–638, https://doi.org/10.1016/j.tcb.2004.09.016.

[45] X. Chen, H. Liu, P.J. Focia, A.H. Shim, X. He, Structure of macrophage colony stimulating factor bound to FMS: diverse signaling assemblies of class III receptor tyrosine kinases, Proc. Natl. Acad. Sci. U.S.A. 105 (47) (2008) 18267–18272, https://doi.org/10.1073/pnas.0807762105.

[46] L. Huang, X. Xu, Y. Hao, The possible mechanisms of tumor progression via CSF-1/CSF-1R pathway activation, Rom. J. Morphol. Embryol. 55 (2 Suppl) (2014) 501–506.

[47] Y. Yang, J. Qin, L. Lan, N. Li, C. Wang, P. He, et al., M-CSF cooperating with NFkappaB induces macrophage transformation from M1 to M2 by upregulating c-Jun, Cancer Biol. Ther. 15 (1) (2014) 99–107, https://doi.org/10.4161/cbt.26718.

[48] Y. Li, Y. Zheng, T. Li, Q. Wang, J. Qian, Y. Lu, et al., Chemokines CCL2, 3, 14 stimulate macrophage bone marrow homing, proliferation, and polarization in multiple myeloma, Oncotarget 6 (27) (2015) 24218–24229, https://doi.org/10.18632/oncotarget.4523.

[49] M. Zajkowska, B. Mroczko, Chemokines in primary liver cancer, Int. J. Mol. Sci. 23 (16) (2022), https://doi.org/10.3390/ijms23168846.

[50] P. Marques, S. Barry, E. Carlsen, D. Collier, A. Ronaldson, S. Awad, et al., Chemokines modulate the tumour microenvironment in pituitary neuroendocrine tumours, Acta Neuropathol Commun 7 (1) (2019) 172, https://doi.org/10.1186/s40478-019-0830-3.

[51] A.E. Filderman, A. Bruckner, B.M. Kacinski, N. Deng, H.G. Remold, Macrophage colony-stimulating factor (CSF-1) enhances invasiveness in CSF-1 receptor-positive carcinoma cell lines, Cancer Res. 52 (13) (1992) 3661–3666.

[52] A. Patsialou, J. Wyckoff, Y. Wang, S. Goswami, E.R. Stanley, J.S. Condeelis, Invasion of human breast cancer cells in vivo requires both paracrine and autocrine loops involving the colony-stimulating factor-1 receptor, Cancer Res. 69 (24) (2009) 9498–9506, https://doi.org/10.1158/0008-5472.CAN-09-1868.

[53] S. Goswami, E. Sahai, J.B. Wyckoff, M. Cammer, D. Cox, F.J. Pixley, et al., Macrophages promote the invasion of breast carcinoma cells via a colony-stimulating factor-1/epidermal growth factor paracrine loop, Cancer Res. 65 (12) (2005) 5278–5283, https://doi.org/10.1158/0008-5472.CAN-04-1853.

[54] D. Capece, M. Fischietti, D. Verzella, A. Gaggiano, G. Cicciarelli, A. Tessitore, et al., The inflammatory microenvironment in hepatocellular carcinoma: a pivotal role for tumor-associated macrophages, BioMed Res. Int. 2013 (2013) 187204, https://doi.org/10.1155/2013/187204.

[55] A.J. Fleetwood, T. Lawrence, J.A. Hamilton, A.D. Cook, Granulocyte-macrophage colony-stimulating factor (CSF) and macrophage CSF-dependent macrophage phenotypes display differences in cytokine profiles and transcription factor activities: implications for CSF blockade in inflammation, J. Immunol. 178 (8) (2007) 5245–5252, https://doi.org/10.4049/jimmunol.178.8.5245.

[56] J. Lei, P. Chen, F. Zhang, N. Zhang, J. Zhu, X. Wang, et al., M2 macrophages-derived exosomal microRNA-501-3p promotes the progression of lung cancer via targeting WD repeat domain 82, Cancer Cell Int. 21 (1) (2021) 91, https://doi.org/10.1186/s12935-021-01783-5.

[57] S. Chen, Y. Morine, K. Tokuda, S. Yamada, Y. Saito, M. Nishi, et al., Cancer-associated fibroblast-induced M2-polarized macrophages promote hepatocellular carcinoma progression via the plasminogen activator inhibitor-1 pathway, Int. J. Oncol. 59 (2) (2021), https://doi.org/10.3892/ijo.2021.5239.

[58] J. Yang, C. Pi, G. Wang, Inhibition of PI3K/Akt/mTOR pathway by apigenin induces apoptosis and autophagy in hepatocellular carcinoma cells, Biomed. Pharmacother. 103 (2018) 699–707, https://doi.org/10.1016/j.biopha.2018.04.072.
[59] Y.X. Cheng, R. Liu, Q. Wang, B.S. Li, X.X. Xu, M. Hu, et al., Realgar-induced apoptosis of cervical cancer cell line Siha via cytochrome c release and caspase-3 and caspase-9 activation, Chin. J. Integr. Med. 18 (5) (2012) 359–365, https://doi.org/10.1007/s11655-011-0697-z.
[60] E. Vergadi, E. Ieronymaki, K. Lyroni, K. Vaporidi, C. Tsatsanis, Akt signaling pathway in macrophage activation and M1/M2 polarization, J. Immunol. 198 (3) (2017) 1006–1014, https://doi.org/10.4049/jimmunol.1601515.
[61] S. Bi, Y. Zhang, J. Zhou, Y. Yao, J. Wang, M. Fang, et al., miR-210 promotes hepatocellular carcinoma progression by modulating macrophage autophagy through PI3K/AKT/mTOR signaling, Biochem. Biophys. Res. Commun. 662 (2023) 47–57, https://doi.org/10.1016/j.bbrc.2023.04.055.
[62] X. Wu, Y. Luo, S. Wang, Y. Li, M. Bao, Y. Shang, et al., AKAP12 ameliorates liver injury via targeting PI3K/AKT/PCSK6 pathway, Redox Biol. 53 (2022) 102328, https://doi.org/10.1016/j.redox.2022.102328.
[63] X. Chen, X. Wang, F. Zhu, C. Qian, F. Xu, X. Huang, et al., HBV infection-related PDZK1 plays an oncogenic role by regulating the PI3K-Akt pathway and fatty acid metabolism and enhances immunosuppression, J Immunol Res 2022 (2022) 8785567, https://doi.org/10.1155/2022/8785567.